

## A NOVEL INVESTIGATION BASED ON LATTIC BOLTZMANN THEORY FOR NANOCOMPOSITE FLOW THROUGH A MANIFOLD

T. Jafari Behbahani<sup>1, 2</sup>

<sup>1</sup>Refining Technology Development Division, Research Institute of Petroleum Industry (RIPI),  
P. O. Box 14665-1998, Tehran, Iran, [jafarit@ripi.ir](mailto:jafarit@ripi.ir); <sup>2</sup> Department of Civil Engineering,  
K. N. Toosi University of Technology, Tehran, Iran

Received June 5, 2014, Accepted July 28, 2014

---

### Abstract

In this work, a novel predictive modeling for the dynamic simulation of nanocomposite melt flow through a manifold based on CFD simulations is presented. The manifold is attached to the extruder. The carbon nanotube concentration, and mass flow rate were combined with physical properties of the nanocomposite and are default model parameters.

By modeling the manifold geometry, the appropriate flow boundaries were determined, and a solution matrix is produced. The velocity of simulated flow through this matrix is computed, and the appropriate conversions made to yield the maximum pressure.

**Keywords:** CFD modeling; extruder; nanocomposite; manifold; Lattice Boltzmann.

---

### 1. Introduction

Melt extrusion processes have been used in industrial applications for many years. Starting from the polymer and plastic industry, hot-melt extrusion (HME) has also found numerous applications in pharmaceutical manufacturing practice [1].

The future materials will be lighter, stronger, and multifunctional. It is anticipated that these materials will be achieved through nanotechnology, and presently, many efforts are focused on carbon nanotubes. Carbon nanotubes (CNTs) were discovered in 1991. Both single-walled and multi-walled CNTs demonstrate extraordinary properties, but single walled CNTs being notably superior. This combination of polymer melts and CNTs results in the production of nanocomposites.

A screw extruder is commonly used in polymer processing. The mixing performance of the extruder considerably influences the quality and morphology of the final product. For this reason the flow field in the mixing section has been studied by a number of authors to gain a better understanding of the process. Yao *et al.* [2] used the finite difference method (FDM) to determine the flow field in single-screw extruder geometry. The simulations were shown to be in good agreement with the results of a flow visualisation experiment. Horiguchi *et al.* [3] used the lattice gas method (LGM) to examine the same problem. The LGM results were found to be in good agreement with visualisation experiments. Horiguchi *et al.* [4] also considered a quantitative comparison with theory. They indicated that the LGM produced a more accurate result of the flow field compared to the FDM; however, there was still a discrepancy between the LGM simulation and the analytic expression. Simulations using the lattice Boltzmann model (LBM) were performed by Buick and Cosgorve [5]. The LBM is a simplified kinetic model [6] which has developed from the LGM. Results based on the LBM model are more accurate than results obtained by the LGM model. The LBM model considered the fluid in the single-screw mixer to be a Newtonian fluid. In a Newtonian fluid the viscosity, defined as the ratio of the stress to the velocity gradient of the fluid is constant. In many practical situations the fluid in a single-screw extruder will exhibit non-Newtonian behavior. Non-Newtonian fluids have a viscosity which is not constant; it can vary with shear, temperature or time. In this study, we consider the LBM modeling for modeling of flow in the single screw extruder.

## 2. CFD SIMULATION THEORY: The Lattice Boltzmann models

In recent years, Lattice Boltzmann models (LBMs) have become increasingly popular due to their ease of implementation, extensibility, and computational efficiency. The lattice Boltzmann method is a powerful technique for the computational modeling of a wide variety of complex fluid flow problems including single and multiphase flow in complex geometries. It considers a typical volume element of fluid to be composed of a collection of particles that are represented by a particle velocity distribution function for each fluid component at each grid point. The time is counted in discrete time steps and the fluid particles can collide with each other as they move, possibly under applied forces. The rules governing the collisions are designed such that the time-average motion of the particles is consistent with the Navier-Stokes equation. This method naturally accommodates a variety of boundary conditions such as the pressure drop across the interface between two fluids and wetting effects at a fluid-solid interface. It is an approach that bridges microscopic phenomena with the continuum macroscopic equations. Further, it can model the time evolution of systems [7].

Consequently, Lattice Boltzmann has become a reliable alternative to traditional CFD methods. Traditional CFD relies on kinetic theory to produce continuous macroscopic equations. These continuous equations are then discretized using a mesh, and the complication of transition from continuous to discrete variables can introduce errors, especially in the case of an inadequate mesh [8-9].

In contrast, the Lattice Boltzmann method discretizes variables on a microscopic level by defining particles at discrete locations with discrete velocities at discrete moments in time [10]. Lattice Boltzmann refers to the lattice of nodes employed to solve a given problem and the Boltzmann equation from which the method is derived. In the Boltzmann equation, :

$$\frac{\partial f}{\partial t} + v \frac{\partial f}{\partial x} + F \frac{\partial f}{\partial v} = \Omega(f) \quad (1)$$

$f$  is the probability that a particle will be at a position between  $x$  and  $x + dx$  with a velocity between  $v$  and  $v + dv$  at time  $t$ . Thus,  $f = f(x, v, t)$  where  $x$  and  $v$  are position and velocity vectors, respectively, and  $t$  represents time. In Equation 1,  $F$  is the external force causing the particle motion and  $\Omega(f)$  is the collision operator governing interactions between the particles themselves.

This equation allows an exact realization of particle dynamics and has made Lattice Boltzmann a popular technique for solving small-scale fluid-flow problems.

There are several variations of LBMs, each model representing a flow in a different manner. The D2Q9 model shown in Figure 1 is a two-dimensional model (D2) with nine possible velocity vectors (Q9).

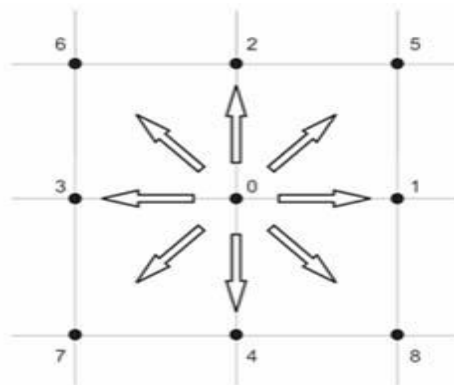


Figure 1. Lattice geometry and velocity vectors of the two-dimensional nine-speed D2Q9 model

At a given time step, the center particle may travel to any of the eight surrounding nodes, or it may remain stationary. Thus, a velocity vector equal to zero constitutes the ninth possible vector.

Lattice Boltzmann can be used to simulate three-dimensional flows with models such as the D3Q15 and D3Q19, which has motion in three dimensions and 15 and 19 associated velocity vectors. In this study we used from D2Q9 model.

Values in the simulation directly associated with the general D2Q9 model are listed in Table 1.

Table 1 D2Q9 Parameters

Parameter	Significance	D2Q9 Value
$c^2$	Speed of Sound Squared	1/3
$(v_i)_x$	x discrete velocity vectors	( 0 1 0 -1 0 1 -1 -1 1)
$(v_i)_y$	y discrete velocity vectors	( 0 0 1 0 -1 1 1 -1 -1)
$w_i$	weighting factor associated with $ v_i ^2 = 0$	4/9
$w_i$	weighting factor associated with $ v_i ^2 = 1$	1/9
$w_i$	weighting factor associated with $ v_i ^2 = 2$	1/36
$w_i$	weighting factor associated with $ v_i ^2 = 3$	1/72

The order of the discrete velocity vectors does not matter. Thus some permutation of the given columns can be used in practice.

### 3. CFD SIMULATION RESULTS AND DISCUSSION

The nanocomposites are produced in sheets, and the ultimate objective is sheets characterized by 1m width, 3mm height, and continuous length. The width and height are governed by a die which can be varied and is located at outlet of the extruder. The die is manufactured in such a way so as to allow for the attachment of a microchannel array [11]. Alignment of the CNTs is required in order to achieve multifunctionality, and this study aims to align the CNTs mechanically through the micro channel array. Shear stresses induced by the manifold and channel walls in the array are to orient the CNTs, and a considerable amount of pressure is required in order to make this feasible [12]. This CFD modeling is to be programmed in MATLAB and based on Lattice Boltzmann principles. Specifically, this modeling will be utilized to calculate the maximum pressure of the laminar flow through the extruder. The user input-variables include polymer selection, carbon nanotube concentration, and mass flow rate.

The polymer options are polystyrene (PS), high-density polyethylene (HDPE), and low-density polyethylene (LDPE) as these are the polymers being investigated with the most frequency.

The six-inch manifold being considered in the analysis is shown in Figure. 2.

Figure 3 contains a view of the cross-section of the manifold. In this figure, the nanocomposites flow over the green and orange areas.

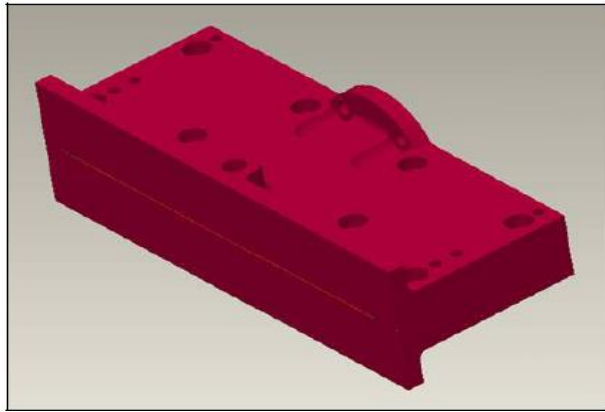


Fig. 2. Model of 6 in Manifold

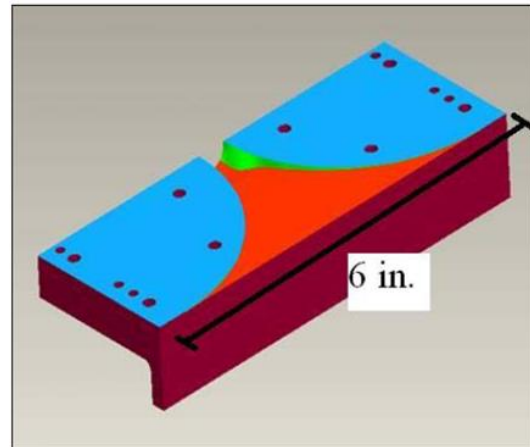


Fig. 3 Cross-Section of ProE Model of 6 in Manifold

The manifold inlet is characterized by a circular cross-sectional area with a diameter of one inch, and this corresponds to the outlet geometry of the extruder. Consequently, all manifolds utilized throughout the oriented nanocomposite extrusion study have this inlet geometry. Nanocomposite sheets are the product of interest; therefore, the geometry of the manifold outlet is rectangular. The cross sectional area between these two planes is continuously decreasing. Knowing the inlet and outlet geometries and the manner of the variation of the cross-sectional area between these planes, it was possible to represent the manifold in modeling.

As a result, the flow exited the manifold through this plane. In the Lattice Boltzmann model used, two walls are required to contain the flow, and only one symmetry plane could be employed. The lower half of the manifold is shown in Figure 4.

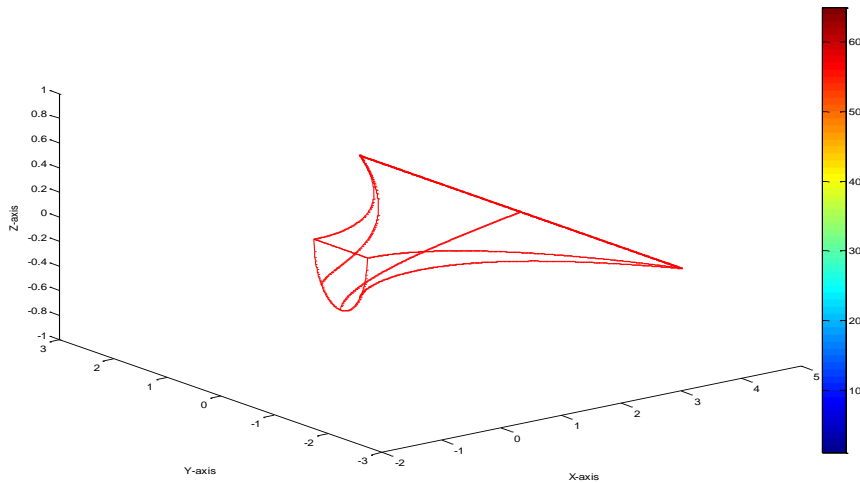


Figure 4 Simulated Model of the Manifold Lower-Half Boundaries

Having the manifold boundaries, arrays of user-specified resolution were swept to map the surfaces. This is shown in Figure 5.

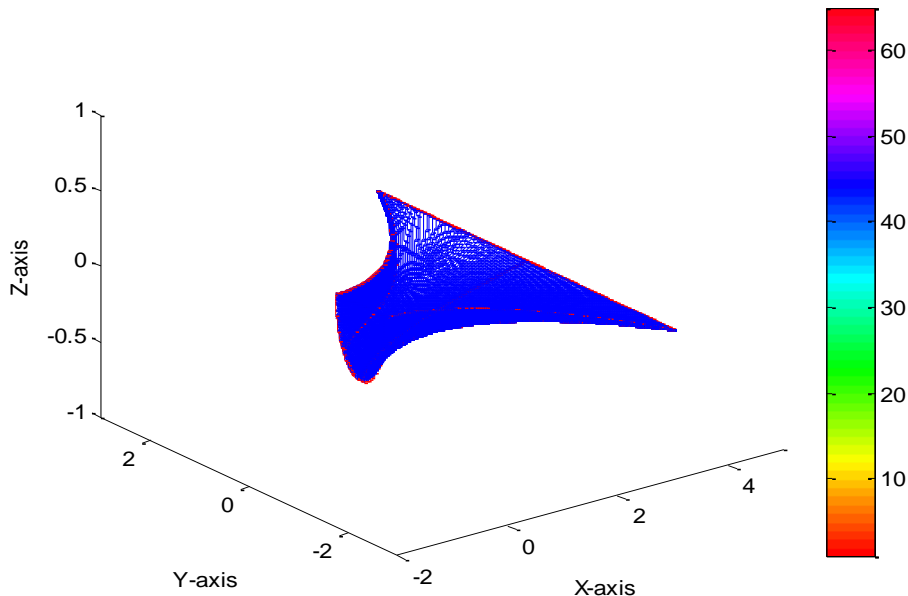


Figure 5 Simulated Model of the Manifold Lower-Half Surfaces

The points generated by these sweeping arrays were used to produce two-dimensional planes extending from the inlet to the outlet. D2Q9 Lattice Boltzmann model was utilized in this simulation.

It was necessary to convert the plane of interest into matrix format to be analyzed with the Lattice Boltzmann method. Each location in the matrix represents a node, which is initially set to a one (flow) or a zero (no flow). The size of the matrix is directly connected to the accuracy of the result. However, a large matrix will also greatly augment the time required to obtain a solution. In this simulation, a 60 x 30 matrix was selected due to the relative

ease of the unit conversion. The 60 rows correlate to the manifold width of 6 in, and the 30 columns represent 3 in length.

The simulation appropriately places ones and zeros in the solution matrix by treating the defining lines of the 2D planes as boundaries [13]. Iterations effectively begin on one side of the matrix with values set to zero. After crossing the boundary into the flow domain, the values are set to one. Upon reaching the opposing boundary, the values are set to zero until the other edge of the matrix is reached. Several fluid parameters are needed to model the flow through this matrix.

As a result, the density and area at the manifold inlet are known, and the velocity at the inlet is determined with the continuity equation. At the outlet, the nanocomposite melt flow is effectively a jet. Thus, assuming atmospheric pressure at the manifold outlet, the static pressure can be determined at the inlet through Bernoulli's Equation.

$$P_{inlet} = P_{outlet} + 1/2 \cdot \rho(V_{outlet}^2 - V_{inlet}^2) \tag{2}$$

These values are then used to determine the pressure gradient inducing the flow.

Upon iteration termination, the simulation compiles a velocity array, and selects the maximum and minimum velocity values. These values are related to pressure through the Navier-Stokes Equation,

$$\rho \left( \frac{\partial V}{\partial t} + V \cdot \nabla \right) = -\nabla P + \rho \cdot g + \mu \cdot \nabla^2 V \tag{3}$$

Upon completion of this calculation, the maximum pressure is determined, and this value is output to the screen.

The simulation was designed to accept any combination of variable values; thus, the potential quantity of results is considerable.

In addition to detailing the maximum pressure throughout the manifold, plots of the solution matrix geometry, fluid obstacles, and the medial axis are generated with each simulation. The solution matrix geometry is shown in Figure 6. Figure 6 is an image of the solution matrix in its numerical form

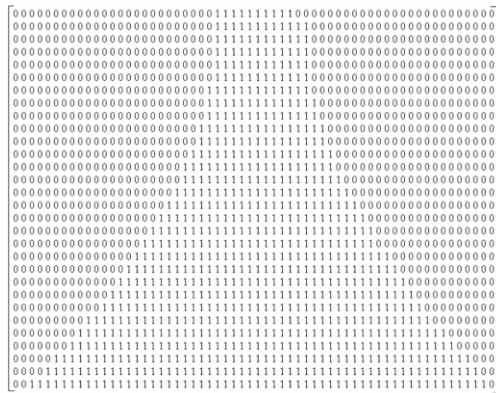


Fig. 6 Solution Matrix in Numerical Form

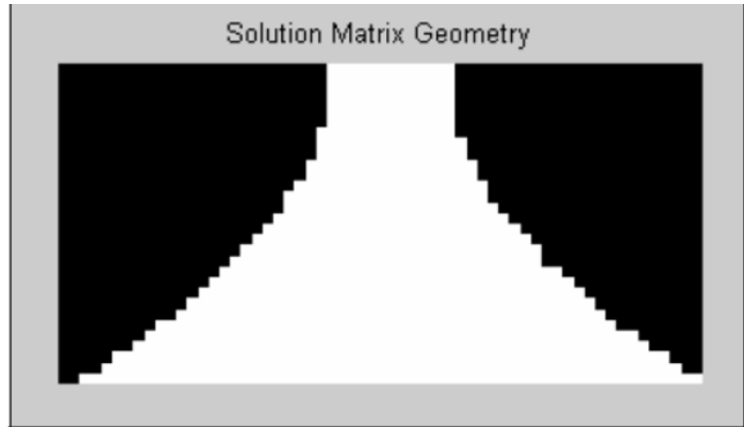


Fig. 7. Simulation output of Solution Matrix Geometry

This is a plot of the solution matrix with the flow area (ones) set to white and the area outside of the flow set to black (zeros). Figure 7 shows the flow boundaries to be jagged, and this is the result of limitations on the size of the solution matrix. The size of the solution matrix is inhibited primarily by computing power. It is expected that in order to obtain acceptably fine boundaries, the size of the solution matrix would have to be increased from 60 x 30 to 6000 x 3000. This would increase the node quantity by a factor of 10,000. An average simulation with the current settings requires approximately two minutes.

Additionally, the simulation outputs images of manifold walls serving as the fluid obstacles and the medial axis associated with the solution matrix. These graphics are included in Figures 8 and 9, respectively.

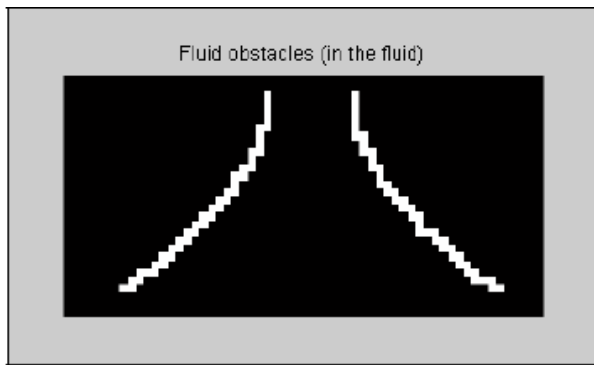


Figure 8. Fluid Obstacles Output

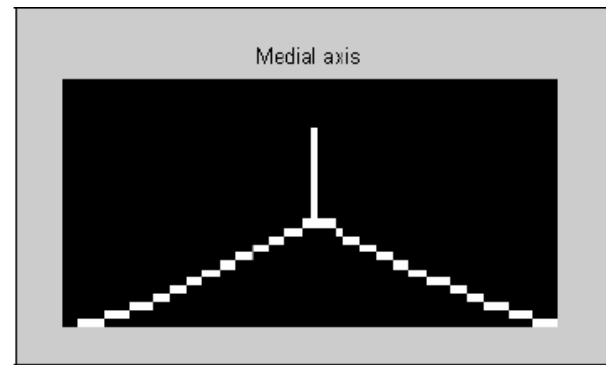


Figure 9. Matrix Medial Axis Output

Assuming reasonable input variables, the convergence variable will be sizeable through the early iterations and quickly approach zero.

#### 4. Conclusions

A D2Q9 Lattice Boltzmann model was used to ascertain the maximum pressure caused by a nanocomposite melt flow through a manifold attached to an extruder. The manifold geometry was constructed in simulation and this geometry was used to acquire the solution matrix. The Lattice Boltzmann model determines the velocity array of the flow through the extruder and calculates the maximum pressure based on this array. The simulation can be predicted the pressure in the manifold.

The predicted maximum pressure patterns are found to be in good agreement in regards to experimental data. It is found that by increasing flow rate, the accuracy of predicted maximum pressure patterns decreases. Also, it is found that by increasing CNT concentration at constant flow rate, the maximum pressure pattern is not change.

#### Nomenclature

Pinlet	The entrance pressure	Voutlet	The outlet velocity
Poutlet	The outlet pressure	$\mu$	Viscosity
Vinlet	The inlet velocity	$\rho$	Density

#### References

- [1] Breitenbach, J.: European Journal of Pharmaceutics and Biopharmaceutics, 2002, 54, 107–117.
- [2] Yao, W.G., Takahashi, K., Abe, Y.: International Polymer Proceedings, 1996, 222–227.
- [3] Yao, W.G., Takahashi, K., Koyama, K., Dai, G.C.: Chemical Engineering Science, 1997, 52,13–21.
- [4] Horiguchi, H., Takahashi, K., Tokota, T.: Journal of Chemical Engineering Japan, 2003, 36, 110–113.
- [5] Buick, J.M., Cosgrove, J.A.: Chemical Engineering Science, 2006, 61, 3323–3326.
- [6] Chen, S., Doolen, G.D.: Annual Review of Fluid Mechanics, 1998, 30, 329–364.
- [7] Abdul, B., Romana Begum, M.: European Journal of Scientific Research, 2008,22, 216-231.
- [8] Chen, A., Sparrow, E.: International Journal of Heat and Mass Transfer, 2009, 52, 1573–1581.
- [9] Motzigemba, M., Broecker, H.C., Prüss, J., Bothe, D., Warnecke, H.J.: Proceedings of the Tenth European Conference, Delft, The Netherlands, 2000, 297-304.
- [10] Dietsche, L.J., Neubauer, A.C.: Chemical Engineering Science, 2009, 64, 4543-4552.
- [11] Radl, S., Tritthart, T., Khinast, J.G.: Chemical Engineering Science, 2010,65,1976-1988.
- [12] Connelly, R. K., L.Kokini, J.: Journal of Food Engineering, 2007,79, 956-969.